Supporting Information

Single-Nanocrystal Photoluminescence Spectroscopy Studies of Plasmon-Multiexciton Interactions at Low Temperature

Young-Shin Park,[1,2] Yagnaseni Ghosh,[2] Ping Xu,[1] Nathan H. Mack,[1] Hsing-Lin Wang,[1] Jennifer. A. Hollingsworth[2] and Han Htoon [1,2]

[1]Chemistry Division, Los Alamos National Laboratory, Los Alamos, New Mexico 87545, USA.
[2]Materials Physics & Applications: Center for Integrated Nanotechnologies, Los Alamos National Laboratory, Los Alamos, New Mexico 87545, USA.

SI 1. Preparation of Silver Nanoflakes Films

Silver films are formed on polyaniline (PANI) films. PANI films were first immersed into citric acid solution (0.25M) for 1 week. The citric acid doped films were then rinsed with water and immersed into freshly prepared aqueous AgNO3 solution for spontaneous formation of silver nanoflakes. The metal growth is stopped by rinsing the films in deionized water. Reaction conditions such as the metal ion concentration and temperature were used to modify the resulting

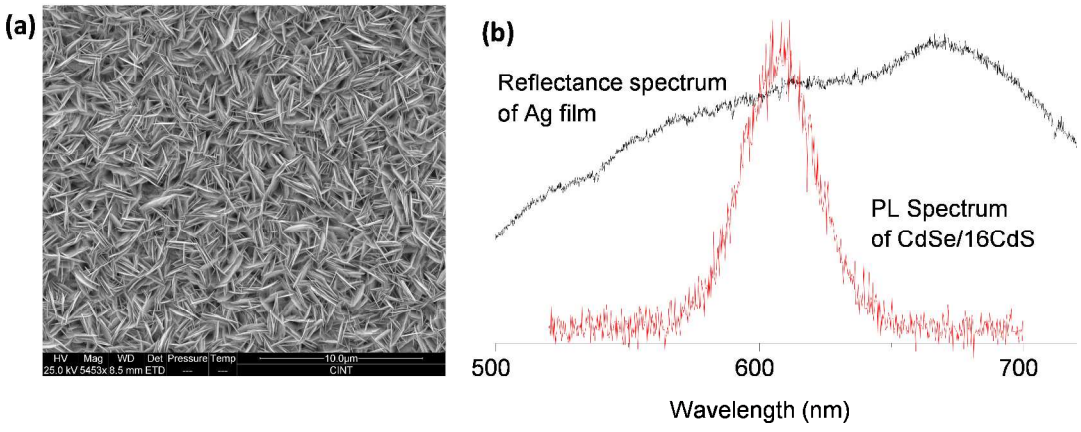

Fig. S1(a) SEM image of the silver nanoflake film. (b) Reflectance spectrum of the silver nanoflake film displayed in comparison with Pl spectrum of a g-NQD at room temperature.

metal nanostructures. A detailed of synthesis and strong surface enhanced Raman activities of these films are reported in reference 26. The films utilized in this experiment is composed of a few micron sized very thin (<100 nm) silver flakes (Fig. S1(a)). Fig. S1(b) displays reflectance spectra of silver film in comparison with RT PL emission spectra of a single g-NQD.

SI 2. The Degree of Photon Bunching in $g^{(2)}$ Functions

Under pulsed excitation condition, the second-order intensity correlation ($g^{(2)}$) function consists of a series of equally-spaced peaks with the time interval determined by a pulse period. The coincidence counts of the side peaks located at non-zero delay time are contributed from two uncorrelated photons emitted at different laser pulses. On the other hand, those of the center peak at zero-time delay come from multiple photons emitted from *ordered* radiative relaxation during a cascade multiexciton decay, for example, triexciton to biexciton to exciton. In $g^{(2)}$ function, the degree of photon bunching (R), defined as the area ratio of the center peak at zero-time delay to one of the side peaks, is given by

$$R = \frac{g^{(2)}(0)}{g^{(2)}(T)} = \frac{\langle n_{ph}(n_{ph}-1)\rangle}{\langle n_{ph}\rangle^2} \tag{S1}$$

where n_{ph} is the photon number emitted from an NQD per an excitation pulse and $\langle\ \rangle$ denotes the average values. When N excitons are excited per one laser pulse, the photon number, n_{ph}, emitted through a cascade relaxation process can be written as,

$$n_{ph} = \sum_{m=1}^{N} \eta_{mX} \tag{S2}$$

where η_{mX} accounts for radiative (η_{mX} =1) or nonradiative (η_{mX} =0) decay process. Assuming that the Poisson distribution function, P(N, $\langle N\rangle$) represents the probability of populating N^{th} MX state at an average exciton occupancy $\langle N\rangle$, the averaged photon number is given by

$$\langle n_{ph}\rangle = \sum_{N=1}^{\infty} P(N,\langle N\rangle) \sum_{m=1}^{N} Q_{mX}\,, \tag{S3}$$

where Q_{mX} is quantum yield of the m-th order exciton. By substituting of $\mathrm{P}(N,\langle N\rangle) = e^{-\langle N\rangle}\langle N\rangle^N/N!$ we obtain the side peak area in terms of $\langle N\rangle$, as

$$\langle n_{ph}\rangle^2 = e^{-2\langle N\rangle}\left\{\langle N\rangle Q_{1X} + \frac{1}{2}\langle N\rangle^2(Q_{1X}+Q_{2X}) + \cdots\right\}^2. \tag{S4}$$

In order to obtain the center peak area, we first calculate the product of n_{ph} and (n_{ph} -1), resulting in

$$n_{ph}\left(n_{ph}-1\right) = \sum_{m=1}^{N}\eta_{mX}\left(\sum_{k=1}^{N}\eta_{kX}-1\right) = 2\sum_{m=2}^{N}\eta_{mX}\sum_{k=1}^{m-1}\eta_{kX}. \tag{S5}$$

Here we used $(\eta_{\mathrm{mX}})^2=\eta_{\mathrm{mX}}$. Again considering Poisson distribution functions of exciton population per laser pulse, we obtain the expression of the center peak area as,

$$\begin{aligned}&\langle n_{ph}\left(n_{ph}-1\right)\rangle = \\ &\quad 2e^{-\langle N\rangle}\left\{\frac{1}{2}\langle N\rangle^2 Q_{1X}Q_{2X} + \frac{1}{6}\langle N\rangle^3(Q_{1X}Q_{2X}+Q_{2X}Q_{3X}+Q_{3X}Q_{1X}) + \cdots\right\}.\end{aligned} \tag{S6}$$

Now, we calculate degree of photon bunching for three different cases in the low excitation limit ($\langle N\rangle \ll 1$).

Case I: spectrally integrated PL

In the low excitation limit ($\langle N\rangle \ll 1$), by keeping the leading terms in the Eqs. (S4) and (S6), we have derived

$$R_0 = \left.\frac{\langle n_{ph}(n_{ph}-1)\rangle}{\langle n_{ph}\rangle^2}\right|_{\langle N\rangle\to 0} \approx \frac{\langle N\rangle^2 Q_{1X}Q_{2X}}{\langle N\rangle^2 Q_{1X}^2} = \frac{Q_{2X}}{Q_{1X}} \tag{S7}$$

This expression states that the degree of photon bunching is simply equal to the quantum yield ratio between biexcitons and single excitons.

Case II: cross-correlation of biexciton-exciton emission

We can derive an expression for the degree of photon bunching ($R_{0,X\text{-}BX}$) of cross-correlation $g^{(2)}$ measurements in which we use spectral filters in front of APDs such that one APD detects only SX photons and the other only MX photons. The center peak area in this case is still given by Eq. (S6) but its area is reduced by half due to the use of the filters. For the side peak, the coincidence counts are contributed by photons emitted from SX and BX at different laser pulses. The filters also reduce the coincidence counts of both peaks by half. Therefore, $R_{0,X\text{-}BX}$ can be written as,

$$R_{X-BX} = \frac{1/2\,\langle n_{ph}(n_{ph}-1)\rangle}{1/2\langle n_{ph}\rangle\langle n_{ph}\rangle_{Q_{1X}=0}}\Bigg|_{\langle N\rangle\to 0} \tag{S8}$$

For $\langle N\rangle \to 0$, we can show readily that $R_{X\text{-}BX}$ also follows the inverse scaling (i.e. $1/\langle N\rangle$). .

Case III: auto-correlation of multiexciton emission

This experiment was performed by inserting a short pass filter to completely block off the SX emission. In this case, for $\langle N\rangle << 1$, the side peak areas mainly originate from BX photons at different laser pulses, while the center peak area comes from successively emitted photons, which consists mostly of a triexciton photon followed by a biexciton photon in a cascade relaxation process. By setting Q_{1X} to zero in Eqs. S(4) and S(6) for the insertion of the short pass filter, the degree of photon bunching of multiexciton auto-correlation $g^{(2)}$ function can be obtained as,

$$R_{MX} = \frac{\langle n_{ph}(n_{ph}-1)\rangle}{\langle n_{ph}\rangle^2}\Bigg|_{\substack{\langle N\rangle\to 0 \\ Q_{1X}=0}} \approx \frac{4Q_{3X}}{3Q_{2X}\langle N\rangle} \tag{S9}$$

Note that R_{MX} increases inversely with decreasing $\langle N\rangle$, which can lead to strong bunching for moderate values of Q_{2X} and Q_{3X}.

SI 3. Distributions of τ_{SX} and Rs of $g^{(2)}$ Functions

In Fig. S1, we compare PL lifetime and degree of photon bunching (*R*) for individual g-NQDs measured either on quartz or on Ag film at T=5K. While g-NQDs deposited on different substrates show large variations on PL lifetimes and *R* values, g-NQDs on Ag film normally have faster PL lifetimes (2.1±1.4ns) and larger *R* (0.66±0.21) compared to g-NQDs on quartz (9.1±3.8ns and 0.35±0.15). We also observed the trend that *R* increases with the decrease of PL lifetimes as shown in Fig. S1(a). A similar enhancement of R values and variation trend are also observed in our room temperature study reported in ref. (16). R values as high as 2.0 with the average of 0.9 were reported in that study. This unusual, >1 R values were explained as a consequence of metal induced PL quenching that exhibits linear scaling with exciton multiplicity, and dominates over both radiative and AR recombinations. We also observed much longer and more widely distributed τ_{SX}s of (49±24 ns) for reference g-NQDs at RT suggesting that the radiative recombination process become much more efficient at low T. Metal induced PL quenching, as a result, can no longer dominate over the radiative recombination process at low T. Analyses of ref. 16 shows that R values under this condition reduce to values below 1.

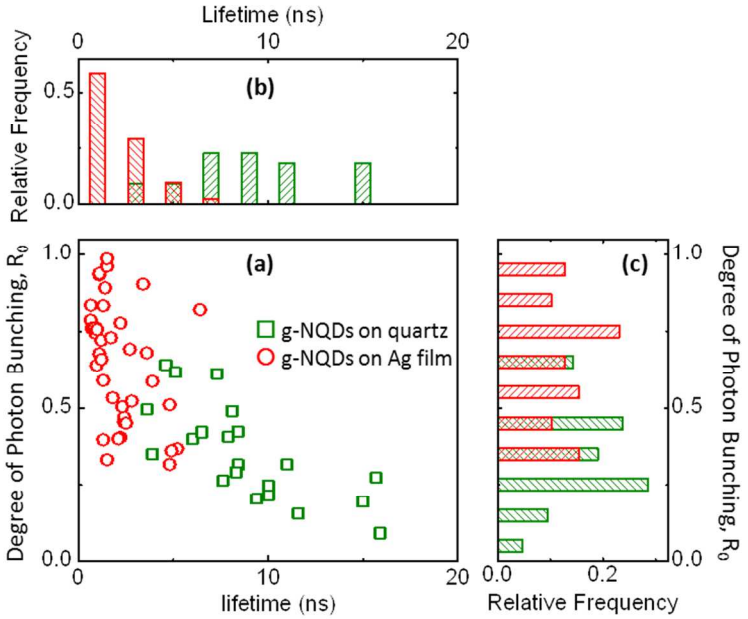

Figure S2. (a) Inverse relationship between PL lifetimes and R_0 values. (b) Histograms of (b) PL lifetimes and (a) R_0 values of ~ 60 individual g-NQDs spread on either quartz (green bar) or Ag film (red bar).

SI 4. More Representative Data for Individual g-NQDs on Ag Film

In Fig. S2, we present more representative data from two different g-NQDs on Ag film. Similar to the g-NQD displayed in Fig. 1, the data show development of distinct SX, BX MX peaks in low T PL spectra (Fig. 2(a) and (h)), near complete antibunching in $g^{(2)}$ of SX emission (Fig. 2(c) and (i), lower panel), incomplete antibunching reflecting Q_{BX}/Q_{SX} in $g^{(2)}$ of spectrally integrated PL (Fig. 2(c) and (i), lower panel), asymmetric peaks and strong photon bunching in $g^{(2)}_{SX,BX}$, and inverse scaling of degree of photon bunching with the increase of pump fluence in $g^{(2)}_{SX,BX}$ and $g^{(2)}_{MX}$. More detailed pump fluence dependent $g^{(2)}_{MX}$ measurements were performed to demonstrate a clear $1/\langle N\rangle$ or inverse pump fluence scaling of R and asymptotic approach of R to unity at the high pump fluence (i.e. $\langle N\rangle > 1$) regime (Fig. 2(e) and (l)).

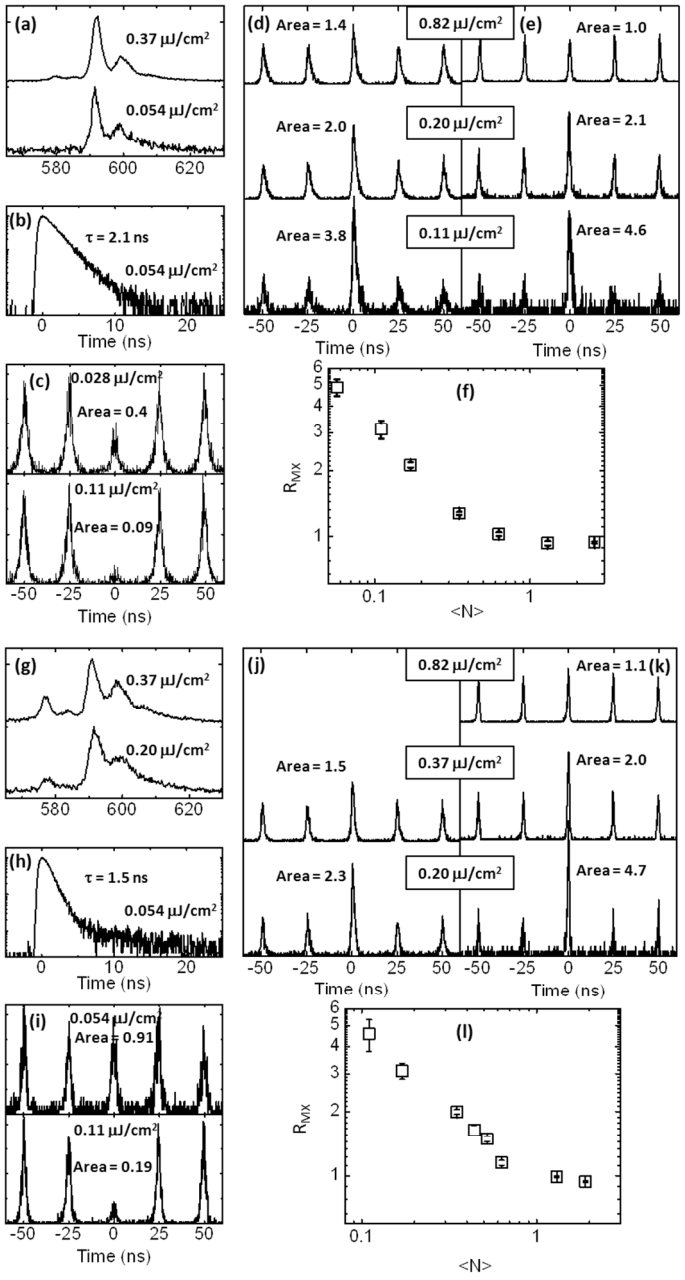

Figure S3. A set of single-dot spectroscopy results obtained at T=5K. (a) PL spectra. (b) PL decay curve. (c) $g^{(2)}$ functions for spectrally integrated PL (upper) and for exciton emission only (lower). (d) Biexciton-exciton cross-correlation $g^{(2)}$ functions. (e) Auto-correlation $g^{(2)}$ functions of multiexciton PL. (f) Area ratio (R) vs. exciton occupancy of multiexciton auto-correlation functions. (h)~(m) Same as for (a)~(f) for other single g-NQD on Ag film.

SI 5. Distribution of τ_{SX}s and f_σs

Based on pump fluence dependence of exciton emission intensity, we estimated absorption enhancement factors for 15 g-NQDs on Ag film that turned out to vary normally in the range of 1~10. The wide distribution of f_σ is expected because the enhancement of the electric field could vary widely between the edges vs. the flat surfaces of the nanoflakes. Enhancement for absorption and emission are expected to be similar due to very wide plasmon resonance of silver nanoflakes. This should lead to some correlation between f_σ and τ_X. However we believe this correlation is washed out by the very wide distribution of τ_Xs and the dot-to-dot variation in the efficiency of PL quenching via charge/energy transfer in our study.

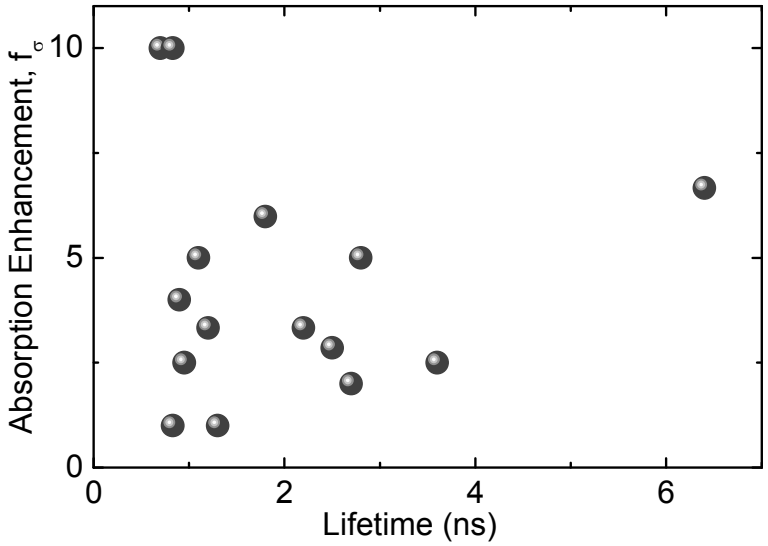

Figure S4. PL lifetimes verses absorption enhancement factors (f_σ).

SI 6. PL Decay Curves and $g^{(2)}$ Functions

In Fig. S4, we display decay dynamics and $g^{(2)}$ functions of five individual g-NQDs whose PL spectra are presented in Fig. 3 in the main text. From the bottom to top, PL decay lifetimes are

found as 8.4, 2.8, 3.6, 1.3, and 0.83 ns, and quantum yield ratios between biexciton and single exciton are calculated as 0.4, 0.5, 0.6, 0.4, and 0.8.

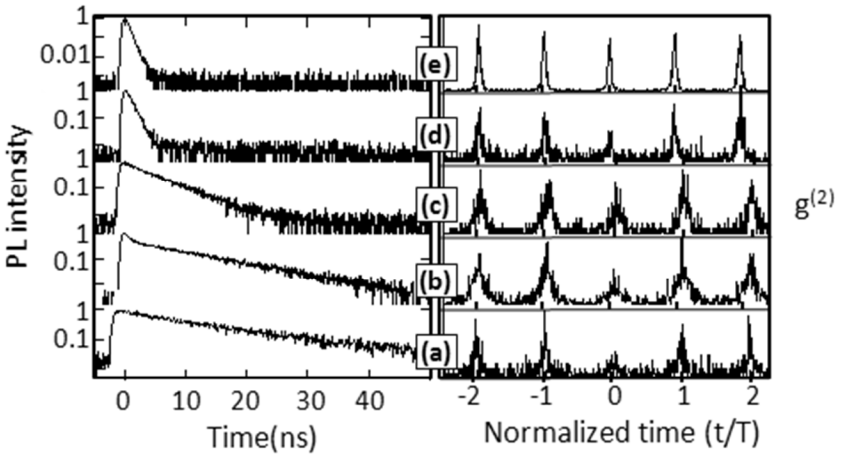

Figure S5. PL decay curves (left) and $g^{(2)}$ functions (right) of five individual g-NQDs that are presented in Fig. 3 in the main text. They are displayed in the same order. Time scales of $g^{(2)}$ functions are normalized with a laser pulse period.

SI 7. Single-exciton and Biexciton PL Intensities

From Eq.(3), single-exciton PL intensity (I_{SX}) is given by,

$$I_{SX} = Q_{SX} \sum_{N=1}^{\infty} P(N, \langle N \rangle) = Q_{SX}\big(1 - P(0, \langle N \rangle)\big) = Q_{SX}\big(1 - e^{-\langle N \rangle}\big) \quad \text{(S9)}$$

For $\langle N \rangle << 1$, I_{SX} is proportional to $\langle N \rangle$, but it saturates to Q_{SX} for large $\langle N \rangle$.Similarly, PL of an m^{th} multiexciton state (I_{mX}) can be described as,

$$I_{mX} = Q_{mX} \sum_{N=m}^{\infty} P(N, \langle N \rangle) \quad \text{(S10)}$$

For $\langle N \rangle << 1$, I_{mX} grows with $\langle N \rangle^m$, but it saturates to Q_{mX} for large $\langle N \rangle$. When experimentally measured PL intensity of SX is normalized to 1 at the saturation, PL of a BX (i.e m=2) normalized using the same factor as SX should saturate to R, which is Q_{BX}/Q_{SX}.